Cyclostationary-based jammer detection for wideband radios using compressed sensing and artificial neural network

Tassadaq Nawaz[1] (iD), Lucio Marcenaro[1] and Carlo S Regazzoni[1,2]

Abstract

Cognitive radio is a promising technology for frequency allocation to improve the spectrum utilization efficiency of licensed bands. However, in recent years, the attention of the researchers is focused on security issues that have to be faced by cognitive radio technology. One of the most important issues consists of radio frequency jamming attacks, where adversaries can use on-the-fly reconfigurability and learning capabilities of cognitive radios in order to devise and deploy advanced jamming tactics. Jamming attacks can noticeably affect the performance of wireless communication systems and can lead to significant overhead in terms of data re-transmission and increased power consumption. In this article, a novel compressed sensing-based jammer detection algorithm is proposed using cyclic spectral analysis and artificial neural networks for wideband cognitive radios. A wideband spectrum is considered that is composed of multiple narrowband signals. Narrowband signals can be legitimate or jamming signals. Compressed sensing is used to reduce the overhead of the analog-to-digital conversion and it allows one to estimate a wideband spectrum with sub-Nyquist rate sampling. After the signal has been estimated, the second-order statistics, namely, spectral correlation function, is computed to extract cyclic features of the wideband signal. Finally, a pre-trained artificial neural network is proposed to classify each narrowband signal as a legitimate or jamming signal. Performances of proposed algorithm are shown with Monte-Carlo simulations under different empirical setups.

Keywords

Wideband radios, jamming attacks, analog-to-digital converter, compressed sensing, spectral correlation function, artificial neural network

Introduction

Over the years, spectrum resources are becoming more and more expensive; for example, industrial, scientific, and medical (ISM) bands are clutched and busier than ever. However, the licensed spectral bands are reported as under-utilized (spectrum holes) by the Primary Users (PUs). Cognitive radio has been proposed to allow opportunistical usage of the licensed bands by Secondary Users (SUs) without causing interference to

[1]Department of Electrical, Electronic, Telecommunications Engineering and Naval Architecture, University of Genova, Genova, Italy
[2]Carlos III University of Madrid, Madrid, Spain

Corresponding author:
Tassadaq Nawaz, Department of Electrical, Electronic, Telecommunications Engineering and Naval Architecture, University of Genova, Via Opera Pia 11, Genova 16145, Italy.
Email: tassadaq.nawaz@ginevra.dibe.unige.it

PUs. This is one of the reasons why cognitive radio has obtained great attention from wireless communication community in recent years. A cognitive radio dynamically interacts with the environment, and it adapts the operating parameters according to the purpose of dynamic spectrum access/opportunistic spectrum access (DSA/OSA).[1,2] In order to discover spectrum holes, spectrum sensing is the primary task needed to be performed.[3]

In the literature, various spectrum detectors have been proposed for cognitive radios, such as matched filter detector (MFD), energy detector (ED), and cyclostationary feature detector (CFD).[4] The MFD can detect the primary signals with good performances, but the overall prior knowledge is needed for the PU's signal. Furthermore, MFD performances degrade in non-stationary environments. The ED is easy to implement, and usually, it shows good performances in low-noise environments. ED is included in the IEEE 802.22 standard for spectrum sensing. However, it fails at low signal-to-noise ratios (SNRs). In most cases, spectrum sensing is needed to detect the weak primary signals accurately. Therefore, another typical spectrum detector called CFD has been proposed to significantly improve the detection rate of the PU signals. CFD is able to accurately detect and even classify the primary signals' different modulations under low SNR conditions, thanks to its cyclic frequency features. Such performances are achieved at the cost of increased implementation complexity. CFD uses the cyclostationarity of the modulated primary signals by detecting spectral peaks by means of the spectral correlation function (SCF) or spectral coherence function (SOF),[5–7] which are sparse in both angular (f) and cyclic (α) frequency domains. Furthermore, it has been used as a robust tool for signal classification when the carrier frequency and bandwidth information are unavailable.[8–10] A comparison of most common methods in terms of complexity and accuracy can be found in Yucek and Arslan.[11] Figure 1 proposes a comparison between different sensing methods taking into account their accuracy and complexity.[11]

When cognitive radios are operating on a wideband (from few hundred MHz to several GHz), the sensing task becomes more complex. A large overhead is imposed to the spectrum sensing system due to the high-rate sampling. Analog-to-digital (A/D) converter and heavy memory usage are particularly affected. Compressive sensing (CS)[12] is an interesting solution to alleviate requirements of high sampling rates provided that the signal is sparse in an appropriate transform domain. Signal sparsity is the main requirement for CS to work, and in the case of cognitive radio networks, it can be a practical assumption because not all frequency bands are occupied all the time in all geographical locations.[1] Therefore, spectrum of the cognitive radio
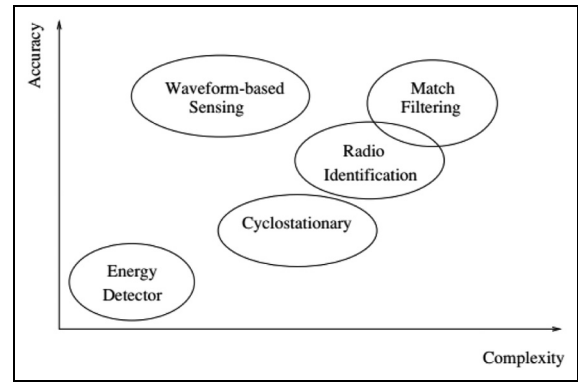

Figure 1. Accuracy versus computational complexity of spectrum sensing detectors.

network can be considered sparse in the frequency domain due to low occupancy by the PUs. CS requires non-linear optimization to find an optimal solution through signal estimation, and this could be achieved by means of greedy algorithms such as Matching Pursuit (MP)[13] or Orthogonal Matching Pursuit (OMP).[14] The other solutions in literature are based on the use of Convex Programming as in Basis Pursuit (BP).[15] Then, CFD needs to estimate the SCF of the received wideband (WB) spectrum from sub-Nyquist samples. A possible approach[16] is to first recover Nyquist samples from sub-Nyquist samples; and then, it is necessary to estimate the SCF and perform feature extraction. To perform Nyquist sample recovery, Mishali and Eldar[17] used modulated wideband converter (MWC). However, a different method is adopted in Tian and Colleagues,[18,19] where they perform SCF estimation directly from sub-Nyquist samples by exploiting the sparsity in two-dimensional SCF domain.

Radio frequency (RF) jamming is the process of transmitting illegitimate signals on one or more occupied channels with the objective of disrupting the communication of the targeted system. Jamming and anti-jamming concepts are as old as radio communications itself, but recent development in cognitive radio technology has permitted devising and deploying of more advanced, self-configurable jamming[20] and anti-jamming[21] solutions. Spectrum sensing plays a key role in designing anti-jamming systems. This spectrum sensing information can be used to detect potential jammers[22] and to take proactive measures to ensure communication continuity and security. Furthermore, an observation set can be maintained over the time and used to employ more effective anti-jamming tactics. For example, when a frequency hopping spread spectrum (FHSS)-based system is used, cognitive radio can modify its hopping sequence to avoid the channels which are occupied by jamming entities.[23] In order to design an appropriate anti-jamming system, there is a need for a reliable jammer detection algorithm.

In this work, we propose a new jammer detection algorithm for WB cognitive radios. The first step is to recover the Nyquist rate WB spectrum, which consists of various narrowband (NB) signals, from sub-Nyquist samples using CS. To this end, conventional BP technique[15] is used. The reconstructed signal is then fed to the CFD to estimate the SCF of the WB signal. The cyclic frequency profile ($\alpha - profile$) is extracted from SCF, and it is used as input feature for an artificial neural network (ANN)-based classifier. Two different ANN-based classifiers are discussed in this work, and one with higher classification performances is used for jammer detection. Based on the ANN classifier, each NB signal is classified either as a legitimate signal or a jamming signal. Finally, the performances of the proposed algorithm are evaluated for various compression ratios and SNRs to observe the effects of parameters on the classification performances.

The rest of this article is organized as follows. Section "System model and problem formulation" presents the system model and problem formulation. Section "Proposed algorithm" outlines cyclostationary spectral analysis, neural network classifier, and proposed algorithm. Experimental results are described in section "Experimental results and discussion," whereas conclusions and future road map are presented in section "Conclusion."

System model and problem formulation

A received WB spectrum of Δ (Hz) is considered here. WB spectrum can be used by various transmitters $n \in \{1, 2, 3, \ldots, N\}$, each one being able to send a bandwidth-separated modulated NB signal at a different carrier frequency. The overall received WB signal is therefore an aggregated time-domain signal which can be written as

$$r(t) = \sum_{n=1}^{N} h_n(t) * s_n(t) + w(t) \quad (1)$$

where $s_n(t)$ denotes the nth transmitted signal, $h_n(t)$ is the channel coefficient between nth transmitter and receiver, * denotes the convolution operation and $w(t)$ is the additive white Gaussian noise (AWGN) with zero mean and power spectral density (PSD) σ_w^2. NB signals are assumed to be generated by different types of modulation schemes characterized by the same bandwidth, such as binary frequency shift keying (BFSK), binary-phase shift keying (BPSK), quadrature amplitude modulation (QAM), quadrature-phase shift keying (QPSK), or any other narrowband modulation scheme as shown in Figure 2(a). WB spectrum can be therefore divided into multiple equal-bandwidth sub-bands (SBs), and
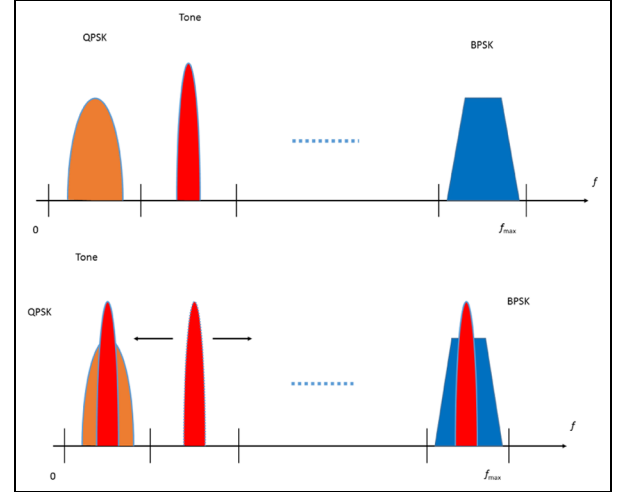

Figure 2. (a) Wideband spectrum divided into multiple sub-bands (SB), and each SB is occupied by a narrowband signal. (b) Narrowband jammer (Tone) jumps to the neighboring SB to jam licit (BPSK or QPSK) signal.

each of these SBs can be occupied by NB signals with no spill-over energy into neighboring SBs.

For our proposed system, the jamming signal is considered as being centered at one of the NB signal frequencies with an equal bandwidth. The jammer is considered to be a cognitive jammer, which can detect and analyze carrier frequencies of legitimate signals to have perfect knowledge of current spectrum occupancy and used modulations. This jammer can jam any of the SBs, if it has higher power than the legitimate signal as depicted in Figure 2(b). The tone jammer is very successful against NB signals, due to the fact that it allows to concentrate all power on a single-data channel. The tone jamming is often considered as the best strategy for jammers with limited transmission power.[24] Let us assume that the targeted signal is QPSK-modulated and uncoded, and that targeted system uses the coherent detection. Then, the error probability (p_e) to either jam the in-phase component (I) or quadrature component (Q) of the targeted signal can be given as follows[22,24]

$$p_e^I = Q\left(\sqrt{\frac{P_r}{P_n}}\left(1 - \sqrt{\frac{2P_j}{P_r}}\text{Sin}(\theta^j)\right)\right)$$
$$p_e^Q = Q\left(\sqrt{\frac{P_r}{P_n}}\left(1 + \sqrt{\frac{2P_j}{P_r}}\text{Cos}(\theta^j)\right)\right) \quad (2)$$

here, P_r is the received power of targeted signal, P_n is thermal noise power, P_j is the jamming signal received power, θ^j is the phase of jamming signal, and Q is the Gaussian Q-function. For our system model, we considered that $P_j >> P_r$, therefore $p_e \approx 100\%$ whenever

jammer transmits on the same channel as the targeted transmitter–receiver pair.

Proposed algorithm

In this section, we first introduce SCF, CS, and ANN, and finally, the new proposed algorithm is presented.

Cyclostationary spectral analysis

A process $r(t)$ is said to be wide-sense cyclostationary with period T_0 if its mean $E[r(t)] = \mu_r(t)$ and autocorrelation $E[r(t)r(t + \tau)] = R_r(t, \tau)$ are both periodic with period T_0

$$M_r(t + T_0) = M_r(t), \quad R_s(t + T_0, \tau) = R_r(t, \tau) \qquad (3)$$

The autocorrelation function of a wide-sense cyclostationary process can be expressed in terms of its Fourier series components

$$R_r(t, \tau) = E[r(t + \tau/2)r^*(t + \tau/2)] \qquad (4)$$

$$R_r(t, \tau) = \sum_\alpha R_r^\alpha e^{j2\pi\alpha t} \qquad (5)$$

where $\alpha = a/T_0$ and a is an integer. $E[\cdot]$ is the expectation operator, α is the cyclic frequency, and $R_r^\alpha(\tau)$ represents the cyclic autocorrelation function (CAF) and gives Fourier components. CAF is given by

$$R_r^\alpha(\tau) = \lim_{T \to \infty} \frac{1}{T} \int_{\frac{-T}{2}}^{\frac{T}{2}} R_r(t, \tau)e^{-j2\pi\alpha t}dt \qquad (6)$$

The Fourier transform of the CAF is known as SCF and is given by

$$S_r^\alpha(f) = \int_{-\infty}^{\infty} R_r^\alpha(\tau)e^{-j2\pi f\tau}d\tau \qquad (7)$$

where α is the cyclic frequency and f is the angular frequency.

The major benefit of spectral correlation is its insensitivity to background noise. Since noise occupies the same spectral band as the signal, there is no way to separate the noise from the signal's PSD. However, as spectral correlation measures the temporal correlation of different frequency components, the noise does not play a significant role in the computation of SCF. The reason behind this is that noise is a wide-sense stationary process, and therefore, the spectral components of noise are uncorrelated in time. This fact allows the spectral correlation of a signal to be accurately computed even at low SNRs. Furthermore, different types of
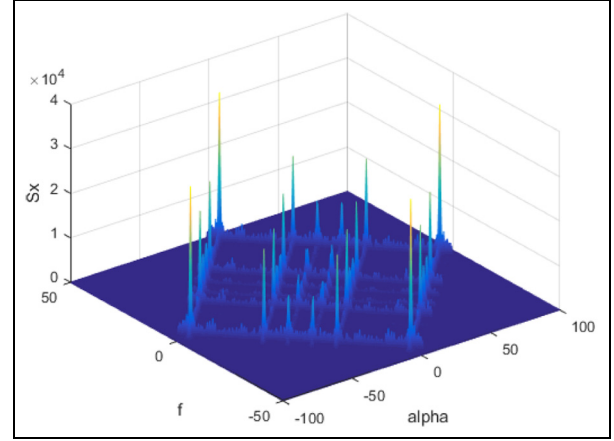

Figure 3. SCF of a wideband spectrum hosting BPSK- and QPSK-modulated signals and a non-modulated tone signal.
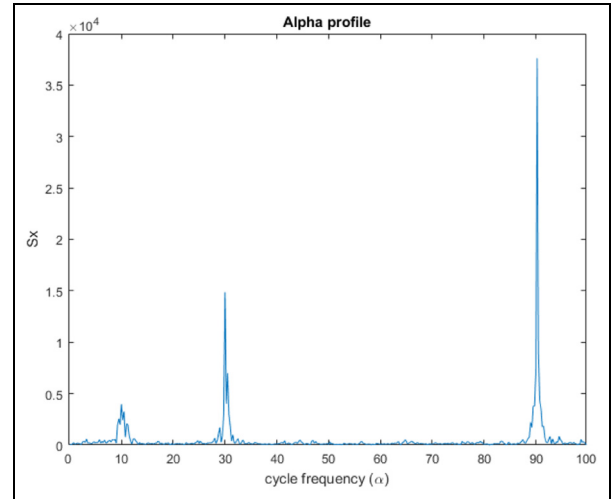

Figure 4. Cyclic frequency profile of a wideband spectrum hosting BPSK and QPSK and a tone signal at different cyclic frequencies.

modulated signals (BPSK, AM, FSK, minimum-shift keying (MSK), QAM, and pulse-amplitude modulation (PAM)) with overlapping power spectral densities have highly distinct SCFs. Our simulations are restricted to the BPSK and QPSK modulation schemes due to the fact that higher order QAM and PSK do not exhibit second-order periodicity but the same features as QPSK. Therefore, these signals can be distinguished by higher order spectral analysis.[25] An example of SCF of a WB signal is depicted in Figure 3.

SCF computation requires large amount of data, which makes it unreasonable for a classifier to operate on it in real time. We used here $\alpha - profile$ as features for classification given in equation (8). The $\alpha - profile$ of SCF for WB signal is shown in Figure 4

$$I(\alpha) = max_f \left[S_r^\alpha \right] \qquad (8)$$

Compressed sensing

This section presents an overview of CS process. The frequency response of the observed WB signal shown in equation (1) can be obtained through N-point discrete Fourier transform (DFT) on $r(t)$ as follows

$$r_f = \sum_{n=1}^{N} D_h^{(n)} S_f^{(n)} + w_f \qquad (9)$$

where r_f is a $N \times 1$ vector of frequency-domain samples, $D_h^{(n)} = diag(h_f^{(n)})$ is an $N \times N$ diagonal channel matrix, and $h_f^{(n)}$, $S_f^{(n)}$ and w_f are the frequency-domain samples of $h_n(t)$, $s_n(t)$, and $w(t)$, respectively. This signal model in equation (9) can be written in more generalized form as follows

$$r_f = H_f \bar{S}_f + w_f \qquad (10)$$

where $\bar{S}_f = [(S_f^{(1)})^T \dots (S_f^{(N)})^T]^T$ is used to denote the spectrum of transmitted signals, and $H_f = [(D_f^{(1)}) \dots (D_f^{(N)})]$ is used to denote the corresponding channel matrix for the receiver. From the above expression, it can be observed that the spectrum sensing task requires to estimate S_f in equation (10) provided we have H_f and $r(t)$. Since the WB signal is available, to alleviate Nyquist rate sampling requirements at the receiver A/D converter, sub-Nyquist signal recovery algorithms can be used. Several computationally efficient techniques, such as BP[15] or OMP,[14] were developed to reliably estimate the received signal sampled at sub-Nyquist sampling rate. The compressed time-domain samples are required to be collected at receiver. Therefore, a CS matrix S_c is constructed to collect a $K \times 1$ sample vector X_t from $r(t)$ as follows

$$x_t = S_c r_t \qquad (11)$$

where S_c is the $k \times n$ projection matrix and r_t is the $N \times 1$ vector of discrete-time representations of $r(t)$ at the Nyquist rate with $K <= N$. There are different schemes introduced in literature for compressive sampler such as non-uniform[26] and random sampler.[27] It is worth noting that $r_t = F_N^{-1} r_f$, and given K compressed measurements, the frequency response $\bar{S}_f$ can now be estimated in equation (11) as follows

$$x_t = S_c^T F_N^{-1} H_f \bar{S}_f + \tilde{w}_f \qquad (12)$$

where $\tilde{w}_f = S_c^T F_N^{-1} w_f$ represents the white Gaussian noise sample vector. In the context of cognitive radio networks, due to low spectrum occupancy by licensed users, the signal vector S_f is sparse in frequency domain. The sparsity of signal vector is measured by

p-norm $||S_f||_p$, $p \in [0, 2)$, where $p = 0$ indicates exact sparsity. Thus, equation (12) is a linear regression problem with signal $\bar{S}_f$ being sparse. The signal $\bar{S}_f$ can be estimated by solving the following linear convex optimization problem

$$\hat{S}_f = arg \min_{\bar{S}_f} ||\bar{S}_f||_1, \quad \text{s.t.} \quad x_t = S_c^T F_N^{-1} H_f \bar{S}_f \qquad (13)$$

This optimization problem can be solved, for example, by means of convex programming as in BP.[15] After the reconstructed Nyquist rate WB signal has been obtained from sub-Nyquist samples, CFD can be used to estimate the SCF of the reconstructed signal. The estimated SCF in this case is definitely dependent on how well the WB signal was estimated from CS, which in turn depends on the sparsity of the signal and the compression rate. The procedure of SCF computation is given in previous section. Then, the features are extracted from obtained SCF of the WB signal and used to train ANN. The $\alpha - profile$ is used as features to train ANN-based classifier. The details of ANN-based classifier are given in the following section.

Neural network classifier

The proposed system uses an ANN as classifier due to the simple implementation and the ability to generalize any parameter, such as carrier frequency, symbol rate, phase offset, and compression ratio. The system is designed to classify signals as BPSK, QPSK, Jammer (single tone), QPSK plus Jammer, and BPSK plus Jammer. This is done with one ANN, which is trained to identify the above five classes of signals. The SCF of WB produces a large amount of data, which makes impossible for a classifier to work on it in near real time. In order to reduce the amount of data for the classification stage, we used $\alpha - profile$ as input features for an ANN. The proposed ANN is composed by 80 inputs related to the $\alpha - profile$, a single hidden layer whose neurons use the hyperbolic tangent sigmoid as a neural transfer function; and an output layer of five neurons relevant to each type of signal is taken into account in this work. The output value is in the range $[0, 1]$ and the output class with the highest value is considered as the class of the signal. ANN is trained based on the scaled conjugate gradient propagation.[28]

The selection of a single hidden layer is proposed due to the classification process simplicity of this particular problem. It was found that with a single hidden layer ANN, an overall accuracy of 90% can be achieved. These results show that adding more hidden layers would increase the training time but without significantly improving overall final performances. According to this, the correct number of neurons can be found by training multiple times 20 different
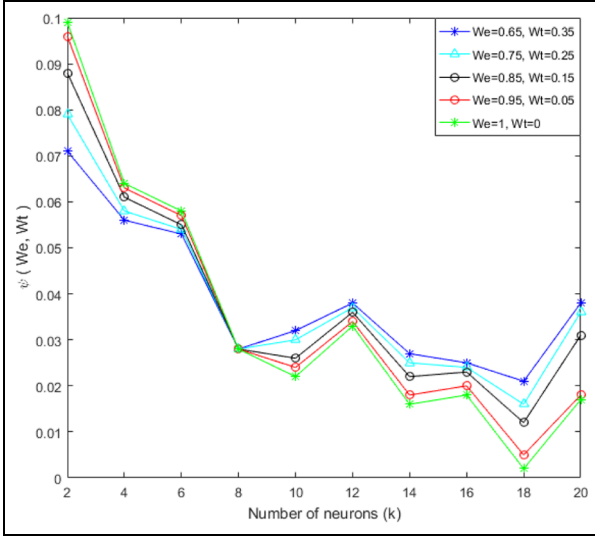
Figure 5. Neural network performance for different number of neurons.
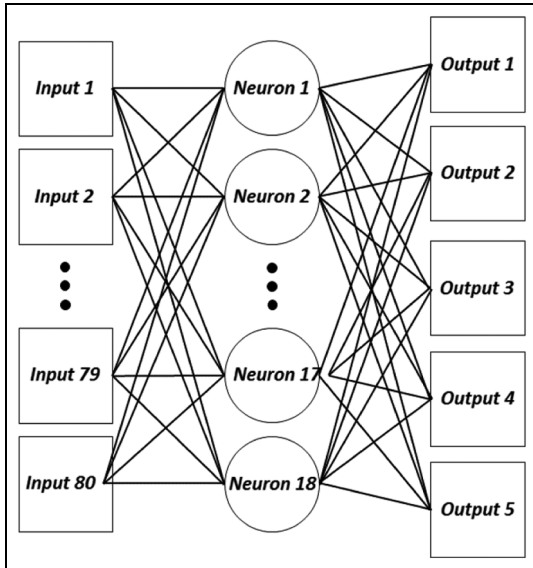

Figure 6. Proposed neural network.

architectures in which the number of neurons in the single layer is varied from 1 to 20. In this way, a number of neurons is selected that does not compromise notably the training time but guarantees robustness at repeating the training process for new ANNs.

A total of 100 trainings are executed for each ANN architecture. For each run, weights are initialized randomly, and a data set composed of 80,000 signals is used in order to train (70%), validate (15%), and test (15%) each architecture. In order to evaluate and compare the overall performance of each architecture, the expression of equation (14) was taken into consideration

$$\Psi_k = W_e(ANN_{er}^k)(std_{er}^k) + W_t(ANN_t^k)(std_t^k) \qquad (14)$$

k is an indicator of the ANN; ANN_{er}^k represents the normalized average error of the 100 trained ANNs for the particular architecture k; ANN_t^k is the normalized average time that a network m took in the training phase; std_{error}^k and std_{time}^k are the standard deviations of the normalized error and training time, respectively, for a particular ANN k; and W_e and W_t are global weights, which indicate the impact that errors and training times have in the performance expression, respectively. Both parameters are related in the following way: $W_e + W_t = 1$. In this work, the overall performance of each architecture k is considered for high values of W_e and therefore low values of W_t. This constraint is considered in this work in order to give more relevance to the error optimization instead of the consumed training time.

From Figure 5, it is possible to observe that the architecture of 18 neurons in the hidden layer achieves the best overall performances in terms of error and training time minimization. According to this, the ANN architecture with 18 neurons that presented the highest performance among the 100 trainings was used for classification purposes, and its results are discussed in next section. The final ANN architecture used in this work is shown in Figure 6.

The proposed algorithm can be summarized as follows: the receiver observes a WB spectrum, which consists of multiple NB signals. The compression ratio is set to a particular value and WB is randomly sampled. Then, the measurement matrix, S_c, is collected at receiver and WB is estimated from sub-Nyquist samples using BP. After this reconstruction, SCF is computed and $\alpha - profile$ features are extracted for different types of signals. Then, these features are fed into previously

---

Algorithm 1 Pseudo-code for proposed algorithm

1:   **function** Jammer Detector
2:       Initialize all SB states to "empty"
3:       Receive the WB signal (1)
4:       Set compression rate $\leftarrow$ K/N
5:       Sample the WB using random sampling (12)
6:       Construct the measurement matrix $\leftarrow S_c$ (12)
7:       Estimate the WB spectrum from compressed samples using BP (14)
8:       Compute the SCF of WB signal (8)
9:       Extract the $\alpha - profile$ (9)
10:         Divide WB into i SBs
11:      **for** $i = 1$ to l, **do**
12:          Feed the $\alpha - profile$ for SB_i to previously trained ANN (15)
13:          Decision $\leftarrow$ Signal type
14:      **end for**
15:      Performance: Classification rates (β) Vs Compression ratios (CR_S)
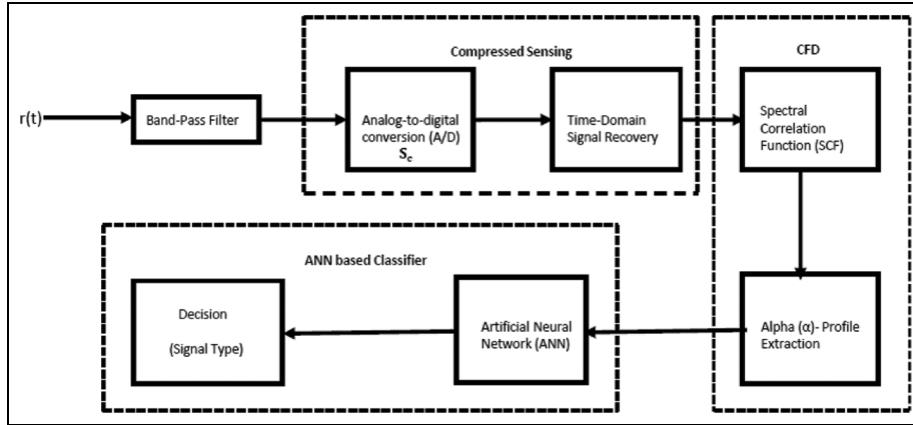16:   Select $\rightarrow$ Best (K/N,SNR)
17:   **end function**

Figure 7. A generic block diagram of the implementation of proposed algorithm.

trained ANN in order to classify NB signals. The ANN classifies each NB signal as "legitimate" or "jamming" signal, and eventually, optimal values for SNR and compression ratio are obtained. The pseudo-code of the proposed algorithm is outlined in Algorithm 1, and a block diagram describing the different steps involved is depicted in Figure 7.

In this work, two different approaches are adopted to train ANN. In first case, the ANN is trained at Nyquist rate, while in second case, it is trained for different compression ratios. In both approaches, the ANN is then tested against different compression ratios.

Experimental results and discussion

A WB spectrum of 50 Hz is assumed to be under observation by a cognitive radio terminal. This WB is divided into five SBs. These SBs can be occupied by NB signals or empty. For testing our proposed algorithm, we assume BPSK and QPSK to be our legitimate signals and single tone (sinusoidal wave) is treated as the jamming signal. The received WB signal is assumed to be affected by AWGN. BP algorithm is used for signal recovery through CS. The performance of proposed system is evaluated for different compression ratios (from $K/N = 0.25$ to $K/N = 1$) at different SNRs (-5 dB, 0 dB, 5 dB, and 10 dB). The system is configured in three different ways: (1) we placed the BPSK signal in SB-1, QPSK in SB-5, and jamming signal in SB-3; (2) BPSK signal is in SB-1, while jamming signal jumps to SB-5 to jam the QPSK signal; and (3) QPSK signal is in SB-5, while jamming signal jumps to SB-1 to jam the BPSK signal. The sampling rate is set at Nyquist rate of 100 Hz. Having the knowledge of the presence of the licit signals, classification is performed at $\alpha \neq 0$, where AWGN exhibits no spectral features.

The Monte-Carlo simulations are run for 1000 iterations for each signal type and for different compression ratios at each SNR. The results are shown for two different types of ANN-based classifiers.

Proposed classifier

Both ANNs, selected based on the process described in neural network classifier section, are trained with 80, 000 signals. First system is trained with full-rate (Nyquist) samples and the second system is trained with various compression ratios. Both the classifiers are trained at different SNRs and carrier frequencies so that the system performance does not depend on the information of these parameters. The proposed system correctly classifies signals with total classification rate of 0.93 and 0.885, respectively.

The performance of both systems is further evaluated for independent test signals, with different compression ratios and SNRs (-5 dB to 10 dB) from training signals. The comparison of overall classification accuracy for two classifiers is given in Figure 8. The plot shows that at low SNRs and low compression ratios, the system trained for different compression ratios outperforms the other system, which is trained only for Nyquist rate samples. For example, at -5 dB, it can be seen that the classification rate is 0.38 for first classifier and 0.65 for second classifier at $K/N = 0.25$. The classification accuracy is increased as K/N is elevated, and it is 0.56, 0.71, 0.82, 0.80, 0.85, and 0.86 at $K/N = 0.40$, 0.55, and 0.70 for two classifiers. However, for higher compression ratios such as $K/N = 0.85, 1$, the performances are approximately the same for both classifiers (0.88 and 0.90). The second classifier, which is trained for different compression ratios, is selected for jammer detection on the basis of the above considerations.
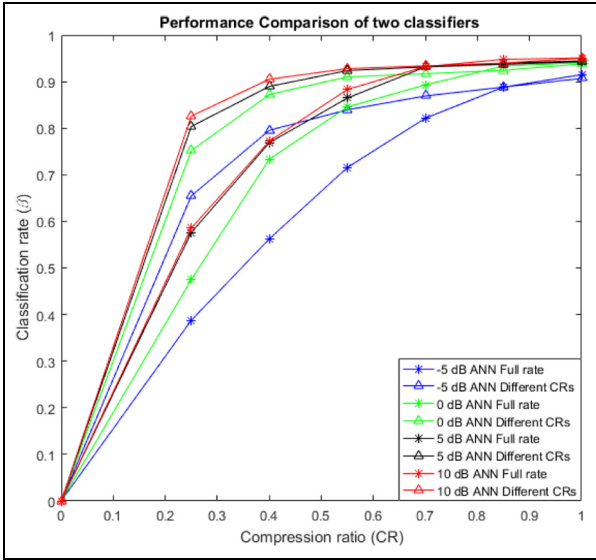
Figure 8. Performance comparison of the two proposed ANN-based classifiers. One is trained at Nyquist rate samples and the other is trained with samples obtained with different compression ratios.
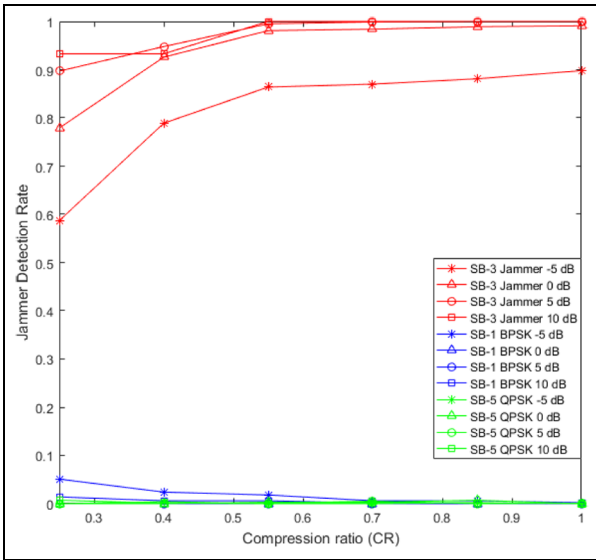

Figure 10. Performance of jammer detection algorithm over various compression ratios and SNRs. SB-1 is occupied by BPSK signal, while jammer has jumped from SB-3 to SB-5 to jam QPSK signal.

Figure 9. Performance of jammer detection algorithm over various compression ratios and SNRs. SB-1 is used by BPSK signal, SB-5 is occupied by QPSK signal, and SB-3 is occupied by jammer.

Jammer detection rate

Figure 9 shows the jammer detection rate versus the compression ratio for occupied SBs. It can be noticed from Figure 9 that at 0 dB, the jammer detection rate in SB-3 is 1 for $K/N = 1.0$, while for that of SB-1 and SB-5 is approximately 0.0. This means that both in S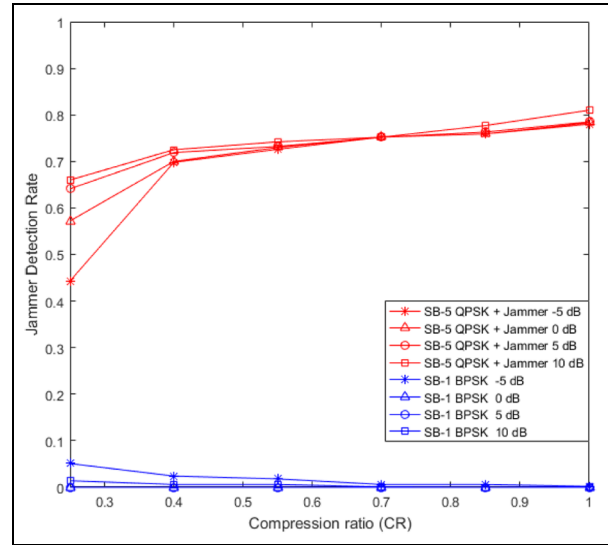B-1 and SB-5, the algorithm correctly classified the legitimate signals (BPSK as BPSK and QPSK as QPSK) with 98% accuracy and misclassified with rate 0.02 BPSK as QPSK and QPSK as BPSK. By decreasing K/N ratio, less samples are available for recovery of signal. As a consequence, the estimated SCF by the CFD is also an approximation. The jammer detection rate is 0.93, even K/N scales down to 0.4. This high accuracy is achieved due to the use of ANN as a classifier and training it for various compression ratios. When $K/N = 0.25$, the jammer detection rate is reduced to 0.779, while wrong classification of jammer as BPSK is 0.049 and that of jammer as QPSK is 0.039. It is worth noticing that jammer is classified as BPSK plus jammer for rate of 0.13, which is in fact an illegitimate signal class.

Jammer detection rate versus the compression rate is plotted in Figure 10 for second test configuration where the jammer jumped into SB-5 to jam the licit QPSK signals. It can be seen that the jammer detection rate falls to 0.78 in SB-5 as compared to 1 in SB-3 from first test scenario. It is because the algorithm is now classifying a mixture of jammer and QPSK in SB-5 with a rate of 0.21. The jammer detection rate once again falls as the compression ratio is decreased due to the poor recovery of the WB signal at low compression rates. For instance, at $K/N = 0.40$, the jammer detection rate is approximately 0.7 in SB-5 with wrong classifications as QPSK to be 0.27.

In third test configuration, the jammer jumped to SB-1 in order to jam the BPSK signals. The jammer detection rate in this case is shown in Figure 11. The
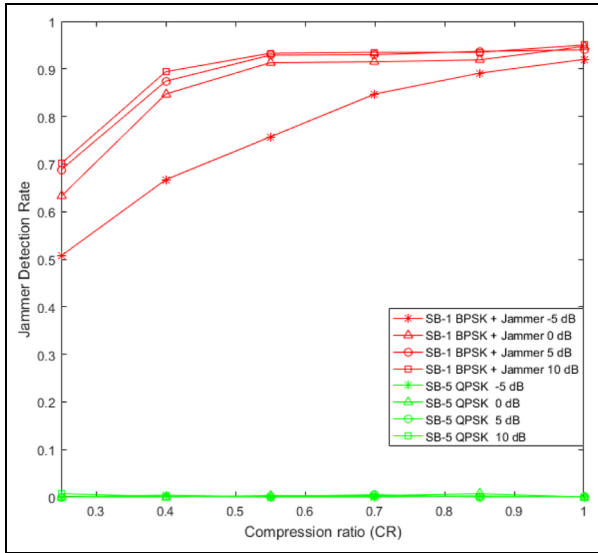
Figure 11. Performance of jammer detection algorithm over various compression ratios and SNRs. SB-5 is occupied by QPSK signal, while jammer has jumped from SB-3 to SB-1 to jam BPSK signal.

jammer detection rate is 0.94 in SB-1 and a 0.06 decrease is observed as compared to 1 in SB-3 from first test scenario. The detection rate is dropped as K/N is decreased, and it is 0.87 at $K/N = 0.40$ and its mistaken rate as BPSK and QPSK is 0.038 and 0.019, respectively.

The proposed algorithm performance is compared with the study by Mughal et al.,[22] and it can be seen from Figure 12 that the usage of ANN not only increases the classification rate but also greatly improves the jammer detection rate. In Mughal et al.,[22] classification was made based on simple comparison of parameters from database. The robustness of the algorithm is shown in Figure 13. It can be seen, even for low compression ratio of 0.4, that the classification rate is approximately 0.87 at 0 dB and 0.8 at −5 dB. This demonstrates that proposed algorithm can efficiently work in an environment where noise level exceeds the signal level. Therefore, this algorithm is robust against noise.

The purpose of the proposed algorithm is also to determine an optimum value for compression ratio and SNR, which reduces the overall cost of the system under consideration. The signals can be further categorized into two broad classes: licit signals (BPSK, QPSK) and illicit signals (Jammer, BPSK plus Jammer, and QPSK plus Jammer). The illicit case is more harmful for any communication system, and the SBs occupied by these signals must be avoided. Table 1 presents the classification rate for $SNR = -5$ dB and $K/N = 0.40$.
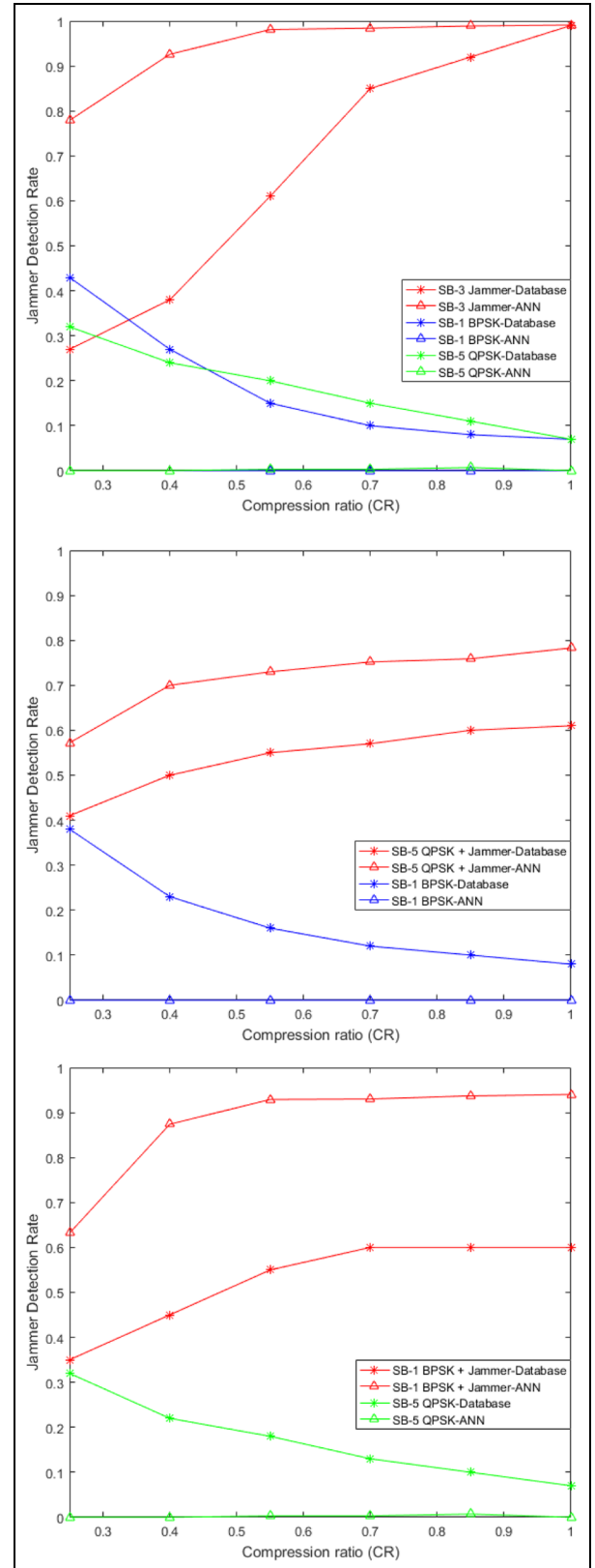

Figure 12. Performance comparison with database matching method.

Table 1. Signal classification for CR = 0.40 at −5 dB.

Test signal	BPSK	QPSK	Jammer	BPSK plus jammer	QPSK plus jammer
BPSK	935	15	24	26	0
QPSK	100	899	4	1	6
Jammer	26	14	789	163	8
BPSK plus jammer	79	18	218	667	18
QPSK plus jammer	2	273	13	14	698

BPSK: binary-phase shift keying; QPSK: quadrature-phase shift keying; CR: cognitive radio.

Table 2. Signal classification for CR = 0.40 at 0 dB.

Test signal	BPSK	QPSK	Jammer	BPSK plus jammer	QPSK plus jammer
BPSK	938	62	0	0	0
QPSK	35	950	0	0	15
Jammer	17	12	926	40	5
BPSK plus jammer	38	19	79	847	17
QPSK plus jammer	2	268	12	18	700

BPSK: binary-phase shift keying; QPSK: quadrature-phase shift keying.
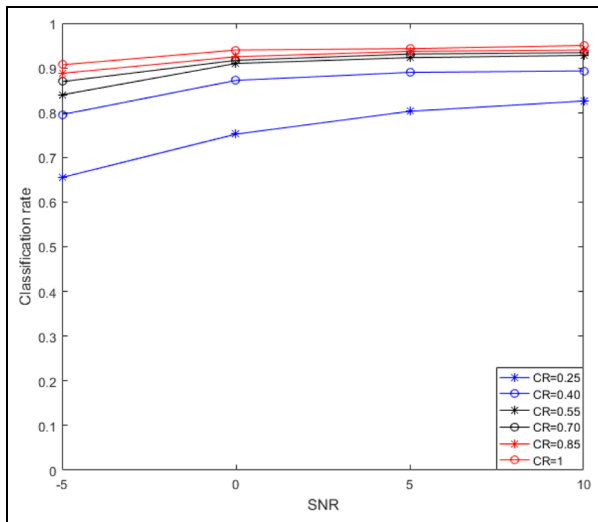
Figure 13. Robustness of proposed algorithm.

The algorithm classified BPSK and QPSK for 95% and 98% as a legitimate signal (BPSK and QPSK) consecutively, while for 5% and 2% algorithm wrongly classified as the jamming signal (Jammer, BPSK plus Jammer and QPSK plus Jammer). Similarly, Jammer, BPSK plus Jammer, and QPSK plus Jammer are correctly classified for 96%, 90% and 73% as illicit signals and wrongly classified as legitimate signals for 4%, 10%, and 27%.

Table 2 shows signal classification rate at SNR 0 dB and $K/N = 0.40$. The BPSK and QPSK are classified 100% and 98.5% as licit users, respectively. Similarly, jammer is correctly detected as illicit signal for 97%.

When the jammer jumps into the band occupied by the BPSK signal, the band is for 94.3% classified as illegitimate band. When the jammer jumps to jam QPSK, the algorithm correctly classifies it as illegitimate signal for 73%.

Therefore, by analyzing Figure 8 and Tables 1 and 2, it can be concluded that a −5 dB and 0.40 would be a smart choice for SNR and compression ratio, which means that this technique is robust to noise and can save up to 60% of sensing energy. Hence, it is definitely an adequate choice for two broad signal classes.

This work considered a constant jammer that sends out random bits without following any medium access control (MAC)-layer protocols. It will be interesting to use this algorithm to detect other types of jammers, for example, deceptive and reactive jammers.[24]

Conclusion

In this article, a cyclic features–based jammer detection algorithm is proposed for WB cognitive radio using ANN. The WB signal is considered to be composed of several NB signals. To reduce the A/D complexity, CS was used for recovering the Nyquist rate samples of the WB signal from sub-Nyquist sampling. The recovered WB signal was then fed to the CFD to compute the SCF of the signal. The $\alpha - profile$ is extracted and fed to two different previously trained ANNs. The classification performances of both the ANN-based classifiers were evaluated at different SNR and compression ratio values. The classifier trained for different compressed ratios is selected on the basis of its good performance

at low SNR and K/N if compared to the classifier trained with Nyquist rate samples. The proposed algorithm appears to perform well at various SNRs down to -5 dB. Since the SCF of different signals are quite different, it appears to be a very effective parameter to use in classification. Furthermore, it is shown that the ANN-based classifier significantly increases the performance when compared to plain database–matching methods.

In the end, algorithm determines the optimum value for compression ratio and SNR in order to reduce the sensing energy and to work in an environment where noise level exceeds the signal level. The algorithm classifies the signals with a high accuracy in noisy channels and can save more than half of the sensing energy. Additionally, such a jammer detection algorithm could be helpful in formulating intelligent anti-jamming strategies for WB cognitive radio systems.

In future work, more sophisticated jamming attacks, such as deceptive and reactive jamming attacks, will be considered. The deceptive jammer is one that transmits regular packets into the channel, following the physical and MAC layer protocol. However, reactive jammer is equipped with sensing ability and only transmits when there is an activity on channel. Furthermore, these jammers may have the learning ability. These types of jamming attacks are hard to detect and hence present potential future research topic.

ORCID iD

Tassadaq Nawaz https://orcid.org/0000-0001-5730-6383

References

1. Mitola J and Maguire GQ. Cognitive radio: making software radios more personal. *IEEE Pers Commun* 1999; 6(4): 13–18.
2. Haykin S. Cognitive radio: brain-empowered wireless communications. *IEEE J Sel Area Comm* 2005; 23(2): 201–220.
3. Yilmaz HB, Tugcu T, Alagoz F, et al. Radio environment map as enabler for practical cognitive radio networks. *IEEE Commun Mag* 2013; 51(12): 162–169.
4. Haykin S, Thomson DJ and Reed JH. Spectrum sensing for cognitive radio. *Proc IEEE* 2009; 97(5): 849–877.
5. Kadjo JM, Yao KC and Mansour A. Blind detection of cyclostationary features in the context of cognitive radio. In: *Proceedings of 2016 IEEE international symposium on signal processing and information technology (ISSPIT)*, Limassol, Cyprus, 12–14 December 2016, pp.150–155. New York: IEEE.
6. Yawada PS and Wei AN. Cyclostationary detection based on non-cooperative spectrum sensing in cognitive radio network. In: *Proceedings of 2016 IEEE international conference on cyber technology in automation, control, and intelligent systems (CYBER)*, Chengdu, China, 19–22 June 2016, pp.184–187. New York: IEEE.
7. Ansari AH and Gulhane SM. Investigation of ROC parameters using Monte Carlo simulation in cyclostationary and energy detection spectrum sensing. In: *Proceedings of 2015 international conference on information processing (ICIP)*, Pune, India, 16–19 December 2015, pp.266–271. New York: IEEE.
8. Fehske A, Gaeddert J and Reed JH. A new approach to signal classification using spectral correlation and neural networks. In: *Proceedings of first IEEE international symposium on new frontiers in dynamic spectrum access networks (DySPAN)*, Baltimore, MD, 8–11 November 2005, 144–150. New York: IEEE.
9. Like E, Chakravarthy V, Husnay R, et al. Modulation recognition in multipath fading channels using cyclic spectral analysis. In: *Proceedings of IEEE global telecommunications conference (GLOBECOM)*, New Orleans, LO, 30 November–4 December 2008, 1–6. New York: IEEE.
10. Anyim IG, Chiverton J, Filip M, et al. The implementation of wideband cyclostationary feature detector with receiver constraints. In: *Proceedings of 2017 European conference on networks and communications (EuCNC)*, Oulu, 12–15 June 2017, pp.1–5. New York: IEEE.
11. Yucek T and Arslan H. A survey of spectrum sensing algorithms for cognitive radio applications. *IEEE Commun Surv Tut* 2009; 11(1): 116–130.
12. Donoho DL. Compressed sensing. *IEEE T Inform Theory* 2006; 52(4): 1289–1306.
13. Duarte MF, Wakin MB and Baraniuk RG. Fast reconstruction of piecewise smooth signals from random projections. In: *Proceedings of online proceedings of the workshop on signal processing with adaptative sparse structured representations (SPARS)*, Rennes, November 2005.
14. Tropp JA and Gilbert AC. Signal recovery from random measurements via orthogonal matching pursuit. *IEEE T Inform Theory* 2007; 53(12): 4655–4666.
15. Chen SS, Donoho DL and Saunders MA. Atomic decomposition by basis pursuit. *SIAM J Sci Comput* 1998; 20(1): 33–61.
16. Cohen D, Rebeiz E, Jain V, et al. Cyclostationary feature detection from sub-Nyquist samples. In: *Proceedings of 2011 4th IEEE international workshop on computational advances in multi-sensor adaptive processing (CAMSAP)*,

San Juan, Puerto Rico, 13–16 December 2011, pp.333–336. New York: IEEE.

17. Mishali M and Eldar YC. From theory to practice: sub-Nyquist sampling of sparse wideband analog signals. *IEEE J Sel Top Signa* 2010; 4(2): 375–391.

18. Tian Z. Cyclic feature based wideband spectrum sensing using compressive sampling. In: *Proceedings of IEEE international conference on communications (ICC)*, Kyoto, Japan, 5–9 June 2011, pp.1–5. New York: IEEE.

19. Tian Z, Tafesse Y and Sadler BM. Cyclic feature detection with sub-Nyquist sampling for wideband spectrum sensing. *IEEE J Sel Top Signa* 2012; 6(1): 58–69.

20. Kresimir D. Intelligent cognitive radio jamming—a game-theoretical approach. *EURASIP J Adv Sig Pr* 2014; 2014: 1–16.

21. Kresimir D, Ozair M, Marcenaro L, et al. Cognitive radio as the facilitator for advanced communications electronic warfare solutions. *J Signal Process Sys* 2015; 83(1): 29–44.

22. Mughal MO, Nawaz T, Marcenaro L, et al. Cyclostationary-based jammer detection algorithm for wide-band radios using compressed sensing. In: *Proceedings of 2015 IEEE global conference on signal and information processing (GlobalSIP)*, 14–16 December 2015, pp.280–284. New York: IEEE.

23. Rahman MAJ, Krunz M and Erwin R. Interference mitigation using spectrum sensing dynamic frequency hopping. In: *Proceedings of 2012 IEEE international conference on communications (ICC)*, Ottawa, ON, 10–15 June 2012, pp.4421–4425. New York: IEEE.

24. Kresimir D. *Intelligent jamming and anti-jamming techniques using cognitive radios*. PhD Thesis, University of Genova, Genova, 2014.

25. Gardner WA. Signal interception: a unifying theoretical framework for feature detection. *IEEE T Commun* 1988; 36(8): 897–906.

26. Rashidi M and Mansouri S. Parameter selection in periodic nonuniform sampling of multiband signals. In: *Proceedings of 2010 3rd international symposium on electrical and electronics engineering (ISEEE)*, Galati, Romania, 16–18 September 2010, pp.79–83. New York: IEEE.

27. Yu Z, Hoyos S and Sadler BM. Mixed-signal parallel compressed sensing and reception for cognitive radio. In: *Proceedings of 2008 IEEE international conference on acoustics, speech and signal processing*, Las Vegas, NV, 31 March–4 April 2008, pp.3861–3864. New York: IEEE.

28. Møller M and Fodslette M. A scaled conjugate gradient algorithm for fast supervised learning. *Neural Networks* 1993; 6(4): 525–533.